INTERNATIONAL JOURNAL FOR NUMERICAL METHODS IN FLUIDS, VOL 21, 371–389 (1995)

NUMERICAL SIMULATION OF COMPLEX FLOWS OF NON-NEWTONIAN FLUIDS USING THE STREAM TUBE METHOD AND MEMORY INTEGRAL CONSTITUTIVE EQUATIONS

YVES BEREAUX AND JEAN-ROBERT CLERMONT

Laboratoire de Rhéologie, Domaine Universitaire, BP 53 X, F-38041 Grenoble Cedex, France

SUMMARY

In this paper a memory integral viscoelastic equation is considered for simulating complex flows of non-Newtonian fluids by stream tube analysis. A formalism is developed to take into account co-deformational memory equations in a mapped computational domain where the transformed streamlines are parallel and straight. The particle-tracking problem is avoided. Evolution in time and related kinematic quantities involved with a K-BKZ integral constitutive model are easily taken into account in evaluating the stresses. Successive subdomains, the stream tubes, may be considered for computing the main flow in abrupt axisymmetric contractions from the wall to the central flow region. The 'peripheral stream tube' close to the duct wall is determined by developing a non-conventional modified Hermite element. A mixed formulation is adopted and the relevant non-linear equations are solved numerically by the Levenberg–Marquardt algorithm. Although the singularity at the section of contraction is not involved explicitly, the results obtained for the peripheral stream tube clearly show the singularity effects and the extent of the recirculating zone near the salient corner. The algorithm is stable even at high flow rates and provides satisfactory solutions when compared with similar calculations in the literature.

KEY WORDS axisymmetric contraction; memory integral co-deformational equations; K-BKZ model; streamtube method; Levenberg–Marquardt algorithm; singularity effects

1. INTRODUCTION

Memory integral equations for viscoelastic fluids are generally assumed to be more realistic in predicting the rheological behaviour of polymer melts or solutions. The use of an integral form for the stress tensor $\mathbb{T}$ permits the introduction of various phenomenological parameters, which renders the formulation more attractive to describing complex flow situations in comparison with implicit differential constitutive equations. However, in numerical simulation the use of memory integral models may lead to delicate problems when evaluating the stress tensor, formally written as

$$\mathbb{T}(t) = \mathbb{F}_{\tau=-\infty}^{\tau=t}[\mathbb{K}(\tau)], \tag{1}$$

where $\mathbb{F}_{\tau=0\infty}^{\tau=t}$ denotes a general functional of a kinematic tensor $\mathbb{K}(\tau)$ related to successive positions $\mathbf{X}$ of a material point X on its pathline at different times $\tau \leq t$. Indeed, computing stresses involves determining the particle's kinematic history on a streamline, the points of which do not pass in general through the mesh nodes of the physical flow domain in the context of classical finite difference or finite element techniques (Figure 1). This problem, known as the 'particle-tracking problem', has been solved in two-dimensional flow situations by different approaches that correspond to plane or

CCC 0271–2091/95/050371–19

Received March 1994
Revised November 1994

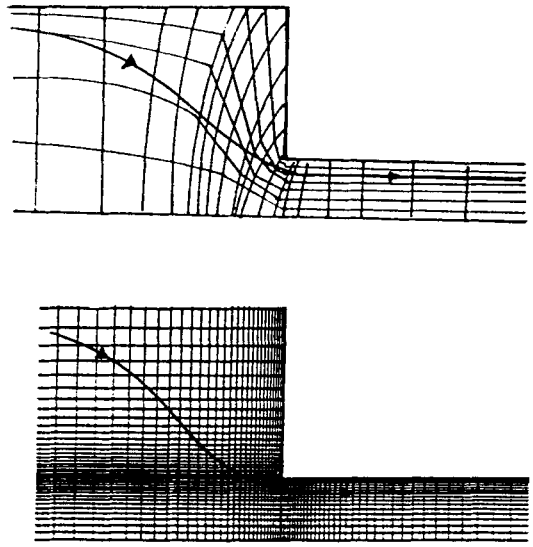

Figure 1. Streamlines in typical meshes used in viscoelastic flow computations

axisymmetric cases. Using general meshes for computing the flow of memory fluids such as Maxwell and Curtiss–Bird fluids, approximations for kinematic histories or drift function methods have been proposed by several authors[1–3] for different constitutive equations. Dupont and Crochet,[4] using a K-BKZ constitutive equation,[5] proposed parametric equations involving a scalar parameter for each element in order to identify the pathline of a material point. Luo and Tanner[6] presented a method in which the integrals of stresses of the same K-BKZ equation were evaluated using a finite element method for flows involving only open streamlines, which were used for building elements updated at each step of the numerical iterative process (Figure 1). Luo an Mitsoulis[7] also adopted the same fluid and the same method for the entry flow in a circular abrupt contraction, setting up conventional finite elements to take into account the closed streamlines of the recirculations encountered in such a flow. The fact that, to our knowledge, few numerical simulations (see e.g. Reference 8) of memory integral viscoelastic 3D flows have been attempted up to the present time is due mainly to significant problems in defining accurate parametric equations for warping curves in order to evaluate kinematic quantities and stresses.

A different approach for computing the flow of memory integral fluids was proposed by Papanastasiou *et al.*[9] For the free surface extrusion problem they proposed a Protean co-ordinate system introduced by Duda and Vrentas[10] and developed by Adachi.[11,12] In the Protean system one co-ordinate is the streamfunction. The work of Papanastasiou *et al.*, in which a K-BKZ integral-type model was adopted, underlined the necessity of using a suitable co-ordinate system for fluids with memory.

The method presented in this paper for evaluating the stress tensor in memory integral models is more closely related to that used with Protean co-ordinates. It refers to the flow analysis introduced some years ago by Clermont,[13] the stream tube method, which may be applied to the study of two- or three-dimensional duct flows[14–16] and pure circulatory or vortex flows.[15] In this approach the unknowns of the problem are, in addition to the pressure p, a one-to-one transformation between the physical flow domain $\mathscr{D}$ (or a subdomain $\mathscr{D}^*$ of $\mathscr{D}$) and a transformed domain $\mathscr{D}'$ (or $\mathscr{D}^{*\prime}$) where the mapped streamlines are parallel and straight (Figure 2). The mapped domain is used as the computational domain. Although this analysis involves considering only open streamlines, it was

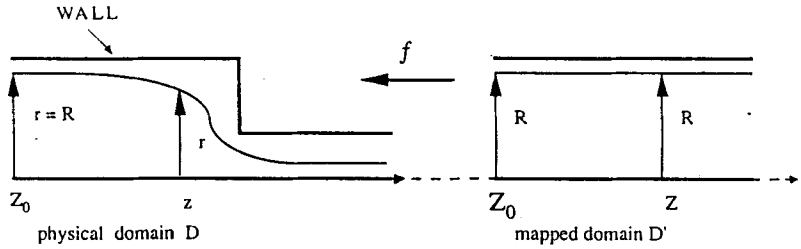

Figure 2. Physical and mapped domains in stream tube analysis for flow in an abrupt contraction involving a recirculation zone

proved that main flows in a duct involving recirculations can still be calculated with stream tube analysis, as was done in a recent numerical work by Clermont and de la Lande.[16]

In stream tube analysis the determination of particle evolution versus time is simplified, since the flow streamlines in the mapped computational domain are rectilinear: in steady 2D and 3D flow situations the mesh points in the computational domain correspond to the successive positions of a particle on its pathline and the particle-tracking problem is avoided. Previous numerical work involving memory integral equations was performed using the stream tube method for free surface[17] and complex duct flows[16] in the two-dimensional case. In both studies a co-rotational modified Goddard–Miller fluid, which was proved to represent the rheological behaviour of a commercial Gedex polystyrene, was selected for the computations. The kinematic tensor used in this model is the rate-of-deformation tensor $\mathbb{D}$, which is expressed in two-dimensional flow situations in terms of first and second derivatives of the mapping function to be determined.

In this paper the K-BKZ memory integral model, which involves the respective co-deformational kinematic Cauchy and Finger tensors $\mathbb{C}_t$ and $\mathbb{C}_t^{-1}$, is considered. Expressing these tensors in the stream tube formalism requires some analytical work, considered in recent studies by Clermont[18] for general 3D flows and Béreaux[19] for the specific case of the K-BKZ model in 2D flows.

The main goal in the present work is to propose, together with a formalism adapted to stream tube analysis, a numerical method which enables efficient computation of axisymmetric entry flows of fluids obeying co-deformational memory integral equations. As already pointed out in the literature, the K-BKZ integral-type model with several relaxation times selected in this study provides consistent predictions of the behaviour of various polymer solutions (see e.g. Reference 20) and melts (see e.g. Reference 5) in shear and elongation as well as in mixed flows.

The general features of the stream tube method in relation to the co-rotational and co-deformational formalisms are examined in Section 2. The basic elements of the memory integral equation adopted in the numerical simulation of the present study are considered in Section 3. Section 4 presents the governing equations and unknowns in the context of stream tube analysis. An element is defined in Section 5 for approximating the mapping function to be determined in relation to numerical problems arising from the presence of the singularity at the salient corner of the contraction. The procedure for solving the governing equations is also presented. The numerical tests and results for entry flows of the K-BKZ fluid are presented and discussed in Section 6. Concluding remarks are given in Section 7.

2. THE STREAM TUBE METHOD AND THE FORMALISM FOR MEMORY INTEGRAL CONSTITUTIVE EQUATIONS

2.1. Basic elements of the stream tube method

The main features of the stream tube method, discussed more extensively elsewhere,[15,16] are presented briefly here.

(1) In the axisymmetric case the transformation **T** between the physical flow domain $\mathscr{D}$ and its mapped domain $\mathscr{D}'$ in which the transformed streamlines are parallel and straight may be expressed by the relations (Figure 2)

$$r = f(R, Z), \qquad \theta = \Theta, \qquad z = Z, \tag{2}$$

where (r, θ, z) and (R, Θ, Z) denote the cylindrical variables in the physical and mapped domains respectively. The Jacobian of the transformation, assumed to be one-to-one, is given by the equation

$$|\partial(r, \theta, z)/\partial(R, \Theta, Z)| = f'_R(R, Z). \tag{3}$$

This has to be non-zero, otherwise several values of f would be possible, corresponding to a recirculating flow zone. This case is not investigated in the present flow analysis: only open streamlines are obtained by numerical computation of the mapping function f defined by the basic equations (2). Domain $\mathscr{D}'$ is used as the computational domain. Consequently, the relevant numerical procedure in this paper concerns the calculation of streamlines in the main flow region of a duct as in Reference 16.

(2) The respective natural and reciprocal bases $\mathbf{b}_i$ and $\boldsymbol{\chi}^j$ related to the co-ordinates (R, Θ, Z) may be expressed in terms of the orthnormal frame $\mathbf{e}_i$ corresponding to the cylindrical variables (r, θ, z) by the equations

$$\mathbf{b}_1 = f'_R(R, Z)\mathbf{e}_1, \qquad \mathbf{b}_2 = f(R, Z)\mathbf{e}_2, \qquad \mathbf{b}_3 = f'_Z(R, Z)\mathbf{e}_1 + \mathbf{e}_3, \tag{4}$$

$$\boldsymbol{\chi}^1 = [1/f'_R(R, Z)]\mathbf{e}_1 - [f'_Z(R, Z)/f'_R(R, Z)]\mathbf{e}_3, \qquad \boldsymbol{\chi}^2 = [1/f(R, Z)]\mathbf{e}_2, \qquad \boldsymbol{\chi}^3 = \mathbf{e}_3. \tag{5}$$

(3) The velocity vector $\mathbf{V}(u, v, w)$, which verifies the incompressibility condition from the stream tube formulation, may be given in terms of the mapping function f by the equations

$$u = -f'_Z(R, Z)\Psi^*(R)/[f(R, Z)f'_R(R, Z)], \qquad v = 0, \qquad w = -\Psi^*(R)/[f(R, Z)f'_R(R, Z)]. \tag{6}$$

In equations (6), $\Psi^*(R)$ stands for the R-derivative of the transformed function of the streamfunction $\Psi(r, z)$, given at the upstream section z_0 of the flow domain, where the kinematics are known, by the equation

$$z = z_0,\ R = r: \quad \Psi^*(R) = \mathrm{d}\Psi(r, z_0)/\mathrm{d}r|_{r=R} = \mathrm{d}\left(-\int_0^r \xi w(\xi, z_0)\mathrm{d}\xi\right)/\mathrm{d}r. \tag{7}$$

(4) On the mapped rectilinear pathlines of the transformed domain $\mathscr{D}'$ the evolution in time of a particle X which occupied positions $\mathbf{X}_{t_0}(R, \Theta, Z_{t_0})$ and $\mathbf{X}_\tau(R, \Theta, Z_\tau)$ at respective times t_0 (reference time related to the position $Z_0 = z_0$ of the particle) and τ is given by the equation

$$\tau = t_0 - [1/\psi^*(R)]\int_{Z_0}^{Z_\tau} f(R, \zeta)f'_R(R, \zeta)\,\mathrm{d}\zeta. \tag{8}$$

2.2. The use of the stream tube method in the co-rotational formalism

In the co-rotational formalism the kinematic tensor $\mathbb{K}(\tau)$ of equation (1) is the rate-of-deformation tensor $\mathbb{D}(\tau)$. In order to satisfy the concept of objectivity for the constitutive equation, the tensor $\mathbb{D}(\tau)$ and the corresponding stress tensor are required to be written first in a co-rotational frame (at each time τ), which is relatively simple to determine in the two-dimensional case (see e.g. References 16 and 18). The derivatives of the velocity with variables (R, Z) of the mapped domain $\mathscr{D}'$ are then evaluated in terms of the function f by derivative operators deduced from equations (2). Details on the use of the stream tube method and a co-rotational memory integral equation were presented in a previous work,[16] as already pointed out.

2.3. The stream tube method in the co-deformational formalism

In this formalism the basic kinematic quantities are the displacement functions. This generally means using the respective Cauchy and Finger objective strain tensors $\mathbb{C}_t(\tau)$ and $\mathbb{C}_t^{-1}(\tau)$ which are related to the deformation gradient tensor $\mathbb{F}_{\blacktriangle}(\tau)$ (see e.g. Reference 21) by the equations

$$\mathbb{C}_t(\tau) = {}^{\mathrm{T}}\mathbb{F}_t(\tau)\cdot\mathbb{F}_t(\tau), \qquad \mathbb{C}_t^{-1}(\tau) = [{}^{\mathrm{T}}\mathbb{F}_t(\tau)\cdot\mathbb{F}_t(\tau)]^{-1}, \tag{9}$$

with

$$\mathbb{F}_t(\tau) = [\partial X_\tau^m/\partial X_t^j]. \tag{10}$$

In equation (9) the superscript 'T' denotes the transposition of a tensor.

Starting from Adachi's work,[11,12] it can be shown[18,19] that by using the vector positions $\mathbf{X}_t$ and $\mathbf{X}_\tau$ and equations (4) and (5) related to the natural and reciprocal bases $\mathbf{b}_i$ and χ^j for variables (R, Θ, Z), the deformation gradient tensor may be expressed in the frame corresponding to (R, Θ, Z) by the matrix

$$\mathbb{F}_t(\tau) = \begin{bmatrix} 1 & 0 & 1 \\ 0 & 1 & 0 \\ \partial Z_\tau/\partial R_t & 0 & \partial Z_\tau/\partial R_t \end{bmatrix}, \tag{11}$$

with

$$\partial Z_\tau/\partial Z_t = w(R, Z_t)/w(R, Z_\tau), \qquad \partial Z_\tau/\partial R_t = w(R, Z_\tau)\int_{Z_t}^{Z_\tau} [\partial w(R, Z_\xi)/\partial R]\mathrm{d}\xi/w(R, Z_\tau). \tag{12}$$

Equations (2), (11) and (12) enables the Cauchy and Finger tensor components to be expressed in terms of the mapping function f and its derivatives. The deformation gradient tensor $\mathbb{F}_t(\tau)$ may be computed by using the natural and reciprocal bases given by equations (4) and (5). In cylindrical co-ordinates the matrix components may be written[18,19] as

$$F^{11} = f'_R(R, Z_\tau)/f'_R(R, Z_t) + [f'_Z(R, Z_\tau)/f'_R(R, Z_t)]\partial Z_\tau/\partial R, \tag{13}$$

$$\begin{aligned} F^{13} = &-[f'_R(R, Z_\tau)f'_Z(R, Z_t)]/f'_R(R, Z_t)] \\ &-[f'_Z(R, Z_\tau)f'_Z(R, Z_t)/f'_R(R, Z_t)]\partial Z_\tau/\partial R + f'_Z(R, Z_\tau)\partial Z_\tau/\partial Z_t, \end{aligned} \tag{14}$$

$$F^{22} = -f(R, Z_\tau)/f(R, Z_t), \tag{15}$$

$$\begin{aligned} F^{31} = {} & [1/f'_R(R, Z_t)]\{\{\Psi^*(R)[\mathrm{d}\Psi^*(R)/\mathrm{d}R]/[f(R, Z_\tau)/f'_R(R, Z_t)]\} \\ & \times \int_{Z_t}^{Z_\tau} [f'_Z(r, \zeta)/f'_R(R, \zeta)]\mathrm{d}\zeta - \{1/[f(R, z_t)f'_R(R, Z_\tau)]\}\int_{Z_t}^{Z_\tau} [(f'_R)^2 + (ff''_{R^2})_{(R,\zeta)}\,\mathrm{d}\zeta\Big), \end{aligned} \tag{16}$$

$$\begin{aligned} F^{33} = {} & -[f'_Z(R, Z_t)/f'_R(R, z_t)]\Big(\{\Psi^*(R)[\mathrm{d}\Psi^*(R)/\mathrm{d}R]/[f(R, Z_\tau)f'_R(R, Z_\tau)]\} \\ & \times \int_{Z_T}^{Z_\tau} [f'_Z(R, \zeta)/f'_R(R, \zeta)]\mathrm{d}\zeta - \{1/[f(R, Z_t)'_f R(R, Z_\tau)]\} \\ & \times \int_{Z_T}^{Z_\tau} [(f'_R)^2 + ff''_{R^2}]_{(R,\zeta)}\,\mathrm{d}\zeta\Big) + f(R, Z_t)f'_R(R, Z_t)/[f(R, Z_\tau)f'_R(R, Z_\tau)], \end{aligned} \tag{17}$$

$$F^{12} = F^{21} = F^{23} = F^{32} = 0. \tag{18}$$

It should be pointed out that in stream tube anlaysis the equations (13)–(17) related to the mapped rectilinear streamlines $\mathscr{L}'$ involve the property

$$\forall \mathbf{X}(R, \Theta, Z)_{(\tau)} \in \mathscr{L}' : \quad R = R_\tau. \tag{19}$$

The Cauchy and Finger tensor components in the cylindrical basis $\mathbf{c}_i$ may be evaluated in terms of the mapping function f and its derivatives using equations (9) and (13)–(18).

3. THE MEMORY INTEGRAL EQUATION

The memory integral equation adopted in the present study is the K-BKZ model already used in several numerical works[4,6,8,9] on viscoelastic flow simulation. The equation was initially proposed by Papanastasiou *et al.*[5] in the form

$$\mathbb{T}(t) = \int_{\tau=-\infty}^{8} \sum_{p=1}^{8} (a_p/\lambda_p)\Psi(I_{\mathbb{C}}, I_{\mathbb{C}^{-1}}) \exp[-(t-\tau)/\lambda_p]\mathbb{C}_t^{-1}(\tau)\, d\tau, \tag{20}$$

in which $\Psi(I_{\mathbb{C}}, I_{\mathbb{C}^{-1}})$ denotes a kinematic function expressed[5] by the equation

$$\Psi(I_{\mathbb{C}}, I_{\mathbb{C}^{-1}}) = \alpha/[(\alpha - 3) + \beta I_{\mathbb{C}^{-1}} + (1-\beta)I_{\mathbb{C}}]. \tag{21}$$

In equations (20) and (21), λ_p and a_p are the relaxation times and the relaxation modulus coefficients respectively, α and β are material constants and $I_{\mathbb{C}}$ and $I_{\mathbb{C}^{-1}}$ denote the first invariants of the Cauchy–Green tensor $\mathbb{C}_t(\tau)$ and its inverse $\mathbb{C}_t^{-1}(\tau)$ respectively. The model parameter values adopted in the present study, which were found to correlate satisfactorily with the experimental data of a low-density polyethylene (LDPE) in shear and elongation, are those already used in several simulations of complex flows (see e.g. References 6 and 9). The coefficients are reported in tables given for example by Luo and Mitsoulis.[7] The following remarks are of interest with regard to the use of the present K-BKZ model in relation to previous numerical work[16] involving the stream tube method and the co-rotational memory integral Goddard–Miller equation.

1. While the co-rotational memory integral involved parameter values fitting satisfactorily with data for a Gedex polystyrene with a single relaxation time, the co-deformational integral K-BKZ model adopted here for LDPE is expressed with eight relaxation times. The kinematic tensors involved in the model are given in terms of the mapping function f by more complicated expressions than those used for the rate-of-deformation tensor related to the co-rotational formalism.
2. From a mathematical point of view the integrals considered in memory integral equations require definition of the numerical integration of a function $F(t, \tau)$. Although in the case of the Goddard–Miller equation[16] the function may be written as

$$F(t, \tau) = F_1(t)F_2(\tau), \tag{22}$$

such factorization of the integrands involved in the K-BKZ equation (13) is not possible. More complicated procedures for evaluating the stress tensor components are therefore needed for this co-deformational model.

As will be seen in the next section, these considerations mean that approximating schemes must be defined for the function f which are different from those previously adopted for numerical simulations with the co-rotational viscoelastic equation.

4. GOVERNING EQUATIONS AND UNKNOWNS

According to the basic equations defining the mapping function f, the numerical simulation involves computing the main flow region of the duct, as pointed out previously. Under isothermal conditions, only the momentum conservation equations are to be written. Ignoring body forces and inertia, these equations are given in differential form, using the function f and the spatial variables of the mapped domain $\mathscr{D}'$, by

$$\begin{aligned} &-[1/f'_R(R, Z)]\partial p(R, Z)/\partial R + [1/f'_R(R, Z)]\partial T^{11}(R, Z)/\partial R \\ &\quad - [f'_Z(R, Z)/f'_R(R, Z)]\partial T^{13}(R, Z)/\partial R + \partial T^{13}(R, Z)/\partial Z \\ &\quad + (T^{11} - T^{22})(R, Z)/f(R, Z) = 0, \end{aligned} \tag{23}$$

$$\begin{aligned} &[1/f'_R(R, Z)]\partial T^{13}(R, Z)/\partial R + [f'_Z(R, Z)/f'_R(R, Z)]\partial p(R, Z)/\partial R \\ &\quad - \partial p(R, Z)/\partial Z - [f'_Z(R, Z)/f'_R(R, Z)]\partial T^{33}(R, Z)/\partial R \\ &\quad + \partial T^{33}(R, Z)/\partial Z + T^{13}(R, Z)/f(R, Z) = 0, \end{aligned} \tag{24}$$

where the superscripts of the stress tensor components T^{ij} are still related to $r = 1, \theta = 2$ and $z = 3$. Writing equations (23) and (24) implies the use of the derivative operators

$$\partial/\partial r = [1/f'_R(R,Z)]\partial/\partial R, \qquad \partial/\partial z = -[f'_Z(R,Z)/f'_R(R,Z)]\partial/\partial R + \partial/\partial Z. \tag{25}$$

The main flow region, simply connected with regard to the open streamlines, may be computed by considering successive stream tubes in the mapped computational domain $\mathscr{D}'$ from the wall to the central flow region. This interesting property, which was discussed in previous papers involving the use of stream tube analysis (see e.g. References 16 and 22), entails taking into account the action of the complementary domain of the stream tube under consideration (Figure 3). In the axisymmetric case the

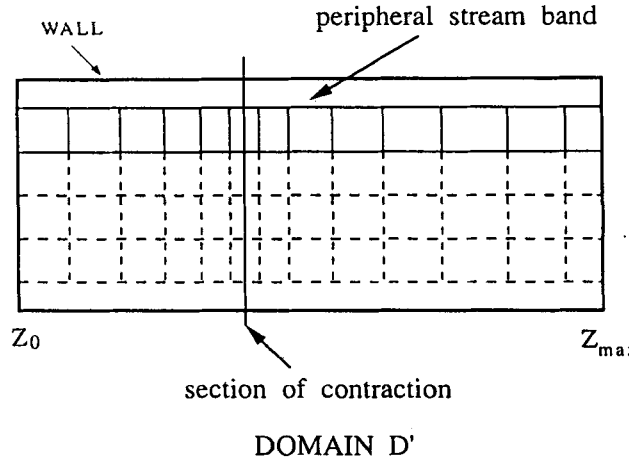

Figure 3. Mapped computational subdomains in $\mathscr{D}'$ for air flow in an abrupt contraction

following scalar integral equation must therefore be written:

$$\left(\int_{\partial\Omega} (-p\mathbb{I} + \mathbb{T}) \cdot \mathbf{n}\, ds\right) \cdot \mathbf{e}_z = 0. \tag{26}$$

This equation corresponds to the global form of the momentum conservation law for a surface $\partial\Omega$ limiting a domain Ω; $\mathbf{n}$ denotes the outer unit normal vector to the surface $\partial\Omega$ and $\mathbb{I}$ is the unit tensor. An extensive description of the procedure defined for the use of this equation was given elsewhere.[16] The quantities involved in equation (26) are expressed as functions of the variables (R, Z) of domain $\mathscr{D}'$.

To compute the flow field, a mixed system of unknowns is considered. This involves the primary unknowns of the problem, namely the transformation function f and the pressure p, as well as the extra-stress tensor components T^{ij} given by integral equations involving functions $\mathscr{H}_p^{ij}(t, \tau)$ related to the kinematic history and material properties of the fluid. According to the constitutive equation (20), these tensor components may be formally written as

$$i, j = 1, 2, 3: \quad T^{ij}(t) = \int_{\tau=-\infty}^{t} \sum_{p=1}^{8} \mathscr{H}_p^{ij}(t, \tau) \exp[-(t-\tau)/\lambda_p]\, d\tau. \tag{27}$$

The stress components are evaluated at points of a mapped rectilinear streamline $\mathscr{L}'$ passing through the position $\mathbf{X}_{t_0}(R, \Theta, Z_{t_0})$ of the upstream Poiseuille flow section limiting the computational domain $\mathscr{D}'$ (Figure 3). Assuming the existence of a fully developed flow at times $t \leq t_0$, the integrals of the form (27) are computed numerically by six-point Gauss–Laguerre formulae, provided that an approximating scheme for the function f and its derivatives is given. Since evaluating the stress tensor involves determining kinematic expressions related to the function f, the following remarks are of interest.

1. Concerning the expressions for the mapping function f and its derivatives:
   (a) for times $\tau \leq t_0 \leq t$ the function f and its first derivatives are given by the simple equations

$$f(R, Z_\tau) = R, \qquad f'_R(R, Z_\tau) = 1, \qquad f'_Z(R, Z_\tau) = 0 \tag{28}$$

   (b) for times $t_0 \leq \tau \leq t$ the function f and its derivatives are evaluated by approximating schemes in the computational flow domain $\mathscr{D}'$.
2. The spatial derivatives $\partial Z_t/\partial Z_\tau$ and $\partial Z_t/\partial R_\tau$ $(\tau \leq t)$ to be used in relation to the deformation gradient components (see equation (12)) may be expressed by the equations

$$\partial Z_t/\partial Z_\tau = R/[f(R, Z_t) f'_R(R, Z_t)], \tag{29}$$

$$\partial Z_t/\partial R_\tau = \{1/[f(r, Z_t) f'_R(R, Z_t)]\}\left(-\Psi^*(R)(t-\tau) + [\Psi^{*2}(R)/R](t_0 - \tau) - \int_{Z_0}^{Z_\tau} \{\partial[f(R, \zeta) f'_R(R, \zeta)]/\partial R\}\, d\zeta\right). \tag{30}$$

   When restricting the computation to a stream tube $\mathscr{R}$ of the main flow region, the governing equations to be solved are
   (a) the dynamic equations (23) and (24)
   (b) the constitutive equations (27)
   (c) the simple boundary condition equations related to data concerning unknowns at the boundaries

(d) two boundary condition equations, of the same type as equation (26), concerning the action of the outer and inner complementary stream tubes;[16] these equations may be considered as constraints for the set of governing equations.

5. DISCRETIZING SCHEMES—ALGORITHM FOR SOLVING THE EQUATIONS

5.1. Approximation of the unknowns

The numerical procedure requires approximating the unknowns in the simple computational domain defined by a stream band $\mathscr{B}'$ in the mapped domain $\mathscr{D}'$ (Figure 3). The stream bands are divided into rectangular elements built on two rectilinear streamlines. The mesh is refined in the vicinity of the contraction section, as is usually the case.

Previous numerical studies involving computation on successive stream tubes have shown that the 'peripheral stream tube' close to the wall of the duct is the one entailing most numerical difficulties.[15,16,22] For flow in all abrupt contraction this boundary is not explicitly taken into account because of the existence of secondary flows close to the wall: the limiting wall only provides known boundary values of the function f. In previous work with the co-rotational memory integral equation the mapping function f, assumed to be quadratic, was approximated in all the stream bands in $\mathscr{D}'$, divided into local elements (e_1) as shown in Figure 4(a), by equations of the form

$$f^{(e_1)}(x, y) = \sum_{i=1}^{6} \Phi_i(x, y) f_i^{(e_1)},$$

where $\Phi_i(x, y)$ are the six basic functions related to the nodal values $f_i^{(e_1)}$. The node locations are also given in Figure 4(a).

The element of type (e_1) was proved to be inadequate with the K-BKZ model: while consistent results were obtained with the co-rotational Goddard–Miller equation, the use of these elements for the peripheral stream band with the co-deformational equation led to oscillations of the computed function f and changes in sign of the Jacobian of the transformation in the vicinity of the contraction section with a refined mesh.

The element (e_2) presented in this paper for interpolation of the function f in the peripheral stream

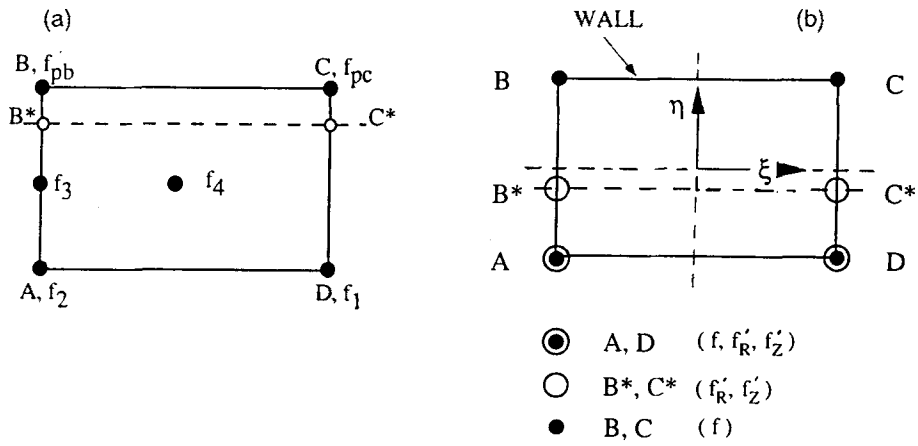

Figure 4. (a) Element of type (e_1) in a stream band. (b) Element of type (e_2) for peripheral stream band in $\mathscr{D}'$

band $\mathscr{B}'$ of $\mathscr{D}'$ is a modified version of a Hermite element[23] and is shown in Figure 4(b). As can be seen, the known values of f are given at wall nodes B and C but are not specified at nodes A* and B* where the first spatial derivatives of f are involved. For points A and B the triplets (f, f'_R, f'_Z) are considered. The function f may then be written with the use of local variables (ξ, η) as

$$f^{(e_2)}(\xi, \eta) = \sum_{j=1}^{12} H_j(\xi, \eta) f_j^{*(e_2)} \tag{31}$$

In equation (31) the quantities f_j^* denote the values of the function f or those of its derivatives f'_R and f'_Z. The correspondence between the basic functions, the quantities f_j^* and the nodes of an element is presented in Table I.

Table 1. Correspondence between geometric nodes, nodal values (f, $\partial f/\partial \xi$ and $\partial f/\partial \zeta$) and basic functions ($H_1$–$H_{12}$) for the modified Hermite element

Geometric nodes	f	$\partial f/\partial \xi$	$\partial f/\partial \eta$
A	H_1	H_2	H_3
D	H_4	H_5	H_6
C	H_7		
B	H_8		
B*		H_9	H_{10}
C*		H_{11}	H_{12}

For the element (e_2) the basic functions H_j may be written as

$$\begin{aligned} H_1(\xi, \eta) = {} & (\eta^2 - 1)[2\eta - 3(\alpha^* - 1)]/[8(3\alpha^* - 1)] - (\eta - 1)/4 \\ & + \xi(\xi^2 - 1)\{1 - (\alpha^* - 1)^2(\eta + 1)/[4(3\alpha^* - 1)]\}/4 \\ & - (\xi/2)\{1 + (\eta + 1)^2(2\eta - 3\alpha^* - 1)/[4(3\alpha^* - 1)]\}, \end{aligned} \tag{32}$$

$$H_2(\xi, \eta) = (\xi^2 - 1)(\eta - \alpha^*)(1 - \xi)/[4(\alpha^* + 1)], \tag{33}$$

$$\begin{aligned} H_3(\xi, \eta) = {} & 2(\eta^2 - 1)[3\alpha^{*2} - 2\alpha^*\eta - 1)](\xi - 1)/[4(3\alpha^* - 1)(\alpha^* + 1)] \\ & - (\alpha^* - 1)^2(\xi^2 - 1)\xi(\eta + 1)/[8(3\alpha^* - 1)], \end{aligned} \tag{34}$$

$$\begin{aligned} H_4(\xi, \eta) = {} & (\eta^2 - 1)[2\eta - 3(\alpha^* - 1)]/[8(3\alpha^* - 1)] - (\eta - 1)/4 \\ & - (\xi/4)(\xi^2 - 1)\{1 - (\alpha^* + 1)^2(\eta + 1)/[4(3\alpha^* - 1)] \\ & + (\xi/2)[1 + (\eta + 1)^2(2\eta - 3\alpha^* - 1)]/[4(3\alpha^* - 1)]\}, \end{aligned} \tag{35}$$

$$H_5(\xi, \eta) = -(\xi^2 - 1)(\eta - \alpha^*)/[4(\alpha^* + 1)], \tag{36}$$

$$H_6(\xi, \eta) = -(\eta^2 - 1)[3\sigma^{*2} - 2\alpha^*(\eta - 1)](\xi + 1)/[4(3\alpha^* - 1)(\alpha^* + 1)] + (\alpha^* - 1)^2(\xi^2 - 1)\xi(\eta + 1)/[8(\alpha^* - 1)], \tag{37}$$

$$H_7(\xi, \eta) = -(\eta^2 - 1)[2\eta - 3(\alpha^* - 1)]/[8(3\alpha^* - 1)] + (\eta + 1)/4 - (\alpha^* + 1)^2\xi(\xi^2 - 1)(\eta + 1)/[16(3\alpha^* - 1)] - \xi(\eta + 1)^2(2\eta - 3\alpha^* - 1)/[8(3\alpha^* - 1)], \tag{38}$$

$$H_8(\xi, \eta) = -(\eta^2 - 1)[2\eta - 3(\alpha^* - 1)]/[8(3\alpha^* - 1)] + (\eta + 1)/4 + (\alpha^* + 1)^2\xi(\xi^2 - 1)(\eta + 1)/[16(3\alpha^* - 1)] + \xi(\eta + 1)^2(2\eta - 3\alpha^* - 1)/[8(3\alpha^* - 1)], \tag{39}$$

$$H_9(\xi, \eta) = (\xi^2 - 1)(\eta + 1)/[4(\alpha^* + 1)], \tag{40}$$

$$H_{10}(\xi, \eta) = (\eta - 1)(\eta + 1)^2(1 - \xi)/[2(3\alpha^* - 1)(\alpha^* + 1)] + \xi(\eta + 1)(\xi^2 - 1)(\alpha^* - 1)/[4(3\alpha^* - 1)], \tag{41}$$

$$H_{11}(\xi, \eta) = (\xi - 1)(\eta + 1)(\xi + 1)^2/[4(\alpha^* + 1)], \tag{42}$$

$$H_{12}(\xi, \eta) = (\eta - 1)(\eta + 1)^2(\xi + 1)/[2(3\alpha^* - 1)(\alpha^* + 1)] - \xi(\eta + 1)(\xi^2 - 1)(\alpha^* - 1)/[4(3\alpha^* - 1)]. \tag{43}$$

In equations (32)–(43) the parameter $\alpha^*(-1 < \alpha^* < 1, \alpha^* \neq 1/3)$ denotes the distance between the ξ-axis and the segment B*C*. The features of element (e_2) are similar to those of the classical two-dimensional Hermite element:

(i) C^0-continuity at the boundaries $\xi = \pm 1$ and $\eta = \pm 1$

(ii) C^1-continuity on the segments $\eta = \pm 1$ of the element and at the geometrical nodes A, B*, C* and D for the partial derivative f'_ξ.

(iii) C^1-continuity on the boundaries $\xi = \pm 1$ and at the geometrical nodes A and D for the partial derivative f'_η.

Starting from properties related to the classical Hermite element (see e.g. Reference 23), it proved possible to evaluate the interpolation error $\boldsymbol{e}$ in the domain $V_r \equiv (e_2)$ of the local variables (ξ, η) for a function $\boldsymbol{U}$ to be approximated along the line $(\xi, \alpha)^*$ where the nodes B*$(-1, \alpha^*)$ and C*$(1, \alpha^*)$ are located; only the nodal values f'_ξ and f'_η are associated with these nodes (Figure 4(b)). The error function $\boldsymbol{e}(\xi, \eta)$ in V_r may be estimated by means of the inequality

$$|\boldsymbol{e}(\xi, \eta)| \leq \{[(\alpha^{*3} + 3\alpha^* - 3\alpha^* + 3)(1 + 2\xi^2)(1 - \xi)^2]\boldsymbol{R}/6 + (\alpha^* + 1)^3(\alpha^* - 1)^2(1 - \xi)^2(1 + \xi)^2]\boldsymbol{S} + (\alpha^* + 1)^3(\alpha^* - 1)^2]\boldsymbol{T}/3\}/[8(1 - 3\alpha)], \tag{44}$$

in which the quanitities $\boldsymbol{R}$, $\boldsymbol{S}$ and $\boldsymbol{T}$ are given by the relations

$$\boldsymbol{R} = \max\left|\partial^4 \boldsymbol{U}/\partial\xi^4\right|_{(\xi, \eta) \in V_r}, \tag{45}$$

$$\boldsymbol{S} = \max\left|\partial^4 \boldsymbol{U}/\partial\xi^2\eta^2\right|_{(\xi,\,\eta)\in V_r}, \tag{46}$$

$$\boldsymbol{T} = \max\left|\partial^4 \boldsymbol{U}/\partial\eta^4\right|_{(\xi,\,\eta)\in V_r}. \tag{47}$$

It may be observed that the error $\boldsymbol{e}(\xi,\eta)$ is smaller when the parameter α^* is close to -1, which corresponds to the node positions of B* and C* shown in Figure 4(b).

The first and second derivatives of the mapping function f can be obtained from derivatives of the basic functions H_j. To compute the pressure p and tensor components T^{ij}, the four nodal values at points A, B*, C* and D of each element are chosen as unknowns. As in previous work,[16] their derivatives in terms of R and Z are then evaluated on the rectangular mesh by using classical finite difference formulae.

5.2. The computational problem—resolution algorithm

While computational procedures are generally set up in such a way that the discretized governing equations of the problem define a closed set of equations, the context of computation on successive stream tubes involves consideration of supplementary equations such as the non-linear boundary condition equation (26). This problem was investigated in previous works (see e.g. References 16 and 22) by means of optimization methods. The equations are written in the form of a problem (P) defined as

$$(\mathrm{P}) \quad \min\{\mathrm{G}(\mathbf{Y}) : \mathbf{Y} \in \mathbb{R}^N\}, \tag{48}$$

corresponding to the set of equations

$$\chi_i(Y_1,\ Y_2,\ \ldots,\ Y_N) = 0, \quad i = 1,\ 2,\ \ldots,\ M, \tag{49}$$

of unknowns $Y_1, Y_2, \ldots, Y_N$. G is a quadratic function given by

$$G(\mathbf{Y}) =^{\mathrm{T}} \boldsymbol{\chi}(\mathbf{Y}) \cdot \boldsymbol{\chi}(\mathbf{Y}) = \sum_{i=1}^{M} \chi_i^2(Y_1,\ Y_2,\ \ldots,\ Y_N). \tag{50}$$

To solve the equations of problem (P), the Levenberg–Marquardt iterative algorithm[24] was adopted. This proved to be solid and efficient for the non-linear problems involved in computing successive subdomains with the stream tube method.[16,22] This algorithm allows a solution $\mathbf{Y}^*$ of (49) to be computed by a combination of two algorithms:

(i) the Newton algorithm, which converges quadratically but requires a good initial estimate $\mathbf{Y}_{[0]}$ of the solution
(ii) the gradient algorithm, which has a linear convergence but converges for a less accurate initial estimate.

In order to compute the unknowns involved in the governing equations, the numerical procedure is carried out by minimizing the quadratic function G defined by equation (50).

6. NUMERICAL RESULTS

The numerical results were obtained with an Apollo 425 workstation using double-precison variables. In relation to the multiple relaxation times of the K-BKZ constitutive equation adopted in the present work, the flow rate was associated with two flow parameters, also used in several other papers[4,6,7]:

(i) the apparent shear rate Γ, defined in the downstream tube by

$$\Gamma = 4\, w_1/r_1, \tag{51}$$

where w_1 denotes the average axial velocity in the downstream tube of radius r_1

(ii) the dimensionless number S_R given by

$$S_R = [N_1/(2T^{13})]_w. \tag{52}$$

In equation (52), N_1 denotes the first normal stress difference and the subscript 'w' indicates that the ratio is considered at the wall of the Poiseuille flow of the downstream tube. The evolution of the parameter S_R versus the apparent shear rate Γ, shown in Figure 5, indicates a slow variation at high shear rates. This should be kept in mind when considering the numerical results expressed in terms of the dimensionless number S_R.

The numerical results are related to the peripheral stream tube of the main flow domain close to the wall. Although the vortex flow zone is not explicitly examined by the stream tube analysis, consideration of this stream tube makes it possible to emphasize the singularity effects due to the salient corner as in previous work with the Goddard–Miller fluid.[16]

The peripheral stream band in the mapped computational domain $\mathscr{D}^*$ involves a number of elements from 20 to 35, the size of which is reduced in the vicinity of the section of contraction in relation to the singularity effectes. In our calculations in the axisymmetric 4/1 contraction the respective upstream and downstream lengths L_u and L_d were defined such that

$$\begin{gathered} L_u/r_1 = 16, \qquad L_d/r_1 = 100 \quad \text{for } S_R \leq 1.7, \\ 100 < L_d/r_1 \leq 250 \quad \text{for } 1.7 \leq S_R \leq 2.67. \end{gathered} \tag{53}$$

The upstream length L_u was the same as that adopted by Luo and Mitsoulis[7] in similar conditions. However, the downstream length L_d required to ensure complete stress relaxation for the K-BKZ viscoelastic model was found to be greater than both that given by those authors and the one reported in our previous work with the single-integral viscoelastic Goddard–Miller equation.[16] For the flow rates considered up to $S_R = 2{\cdot}67$ no convergence problems were encountered with the computational procedure. The convergence criterion, based on the Euclidean norm-of-error ε related to the Levenberg–Marquardt procedure, was given by the equation

$$\varepsilon = \|\Delta G(\mathbf{Y}_{[i]}\|/\|G(\mathbf{Y})_{[i]}\|, \tag{54}$$

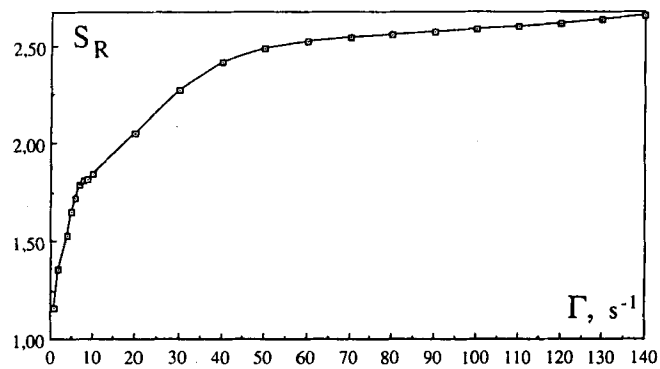

Figure 5. Dimensionless parameter S_R as a function of apparent shear rate Γ

where i denotes the current iteration number and $\Delta G(\mathbf{Y})_{[i]} = G(\mathbf{Y})_{[i]} - G(\mathbf{Y})_{[i-1]}$, the function $G(\mathbf{Y})$ being expressed by equation (50). The relative error ε was generally found to be of the order of 10^{-8}, associated with a function $G(\mathbf{Y})$ of the order of 10^{-6}. An example of the evolution of $G(\mathbf{Y})$ as a function of the number of iterations before convergence is shown in Figure 6. For all the cases considered, the number of iterations was found to be less than 25.

Various tests were run in order to compare the accuracy measured by relative differences between the transformation f, the pressure and the stress components. Given the dimensionless number S_R related to a flow rate, the mesh adopted was that leading to negligible differences in computing the unknowns. In the context of the stream tube method, solving the governing equations in a stream tube reduced the number of unknowns to 400 at the highest flow rates investigated. In contrast with numerical simulations of viscoelastic flow performed in the literature, the solution at a given flow rate did not require intermediate flow calculations at lower values of the parameter S_R. This possibility is to be underlined in relation to

(i) The discretization scheme adopted to compute the unknowns

(ii) smaller relative differences between the problem variables in a stream band of $\mathscr{D}^*$ compared with those involved in a computational method involving the total flow domain

(iii) the efficiency and robustness of the Levenberg–Marquardt algorithm used for solving the equations.

As already pointed out in previous works,[15,16] the existence of the transformation $\mathscr{T}$ for the main flow domain is related to the non-singular character of the Jacobian f'_R of the one-to-one transformation. This made it necessary to consider peripheral stream tubes limited by a streamline $\mathscr{L}^*$ starting at an original abscissa $r^*_{\lim}$ at the upstream Poiseuille flow section, defined such that $(r_0 - r^*_{\lim})/r_0 \leq 0{\cdot}05$ (r_0 is the upstream duct radius), otherwise divergence problems may arise.

Figure 7 illustrates the computed limiting streamline $\mathscr{L}^*$ of the peripheral stream tube with the integral model for $S_R = 1{\cdot}65$, $1{\cdot}84$, $2{\cdot}53$ and $2{\cdot}67$. Although the calculations concerned a subdomain of the main flow region, the shape of the computed limiting streamlines clearly indicates the relative importance of the recirculating flow zone and the evolution of vortex flow near the salient corner of the contraction. Figure 8 shows an example for $S_R = 2{\cdot}53$ of consistent comparisons between the limiting streamline $\mathscr{L}^*$ in the 4/1 contraction determined by solving the equations in the peripheral stream tube and the streamline of the same origin upstream of the contraction determined by Luo and Mitsoulis[7] under the same flow conditions with a finite element method involving the total flow domain.

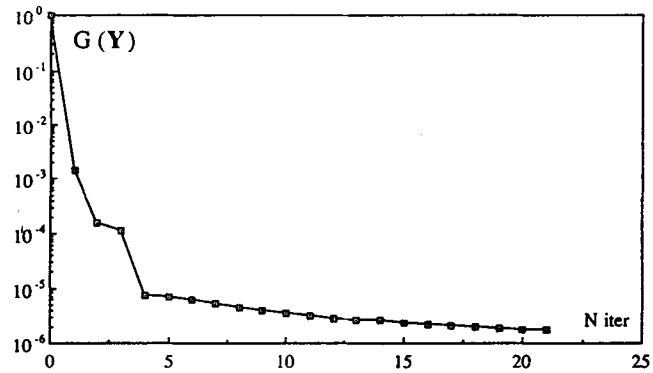

Figure 6. The function G to be minimized as a function of the number of iterations

The stress components along the limiting streamline $\mathscr{L}^*$ corresponding to $S_R = 2{\cdot}67$ are shown in Figure 9(a) and (b). For all the stress components plotted, a peak may be observed in the curves in the vicinity of the contraction section, corresponding to the presence of the salient corner. As can be seen in Figure 9(b), the model exhibits a much greater stress difference $T^{33} - T^{11}$ than the stress difference $T^{11} - T^{22}$, which also relaxes more rapidly. The peak intensity is found to be of the same order of magnitude as that illustrated by numerical results reported by Luo and Mitsoulis.[7]

The importance of singularity effects on the stress components is also illustrated in Figure 10, where the stress distributions T^{13} are plotted at $S_R = 1{\cdot}65$, $2{\cdot}53$ and $2{\cdot}67$. As expected, the magnitude of the stress peaks increases with the dimensionless number S_R.

Computations were also performed for the axisymemtric 8/1 contraction. Results obtained at $S_R = 1{\cdot}84$ are plotted in Figures 11 and 12 for both 4/1 and 8/1 contractions. The computed limiting

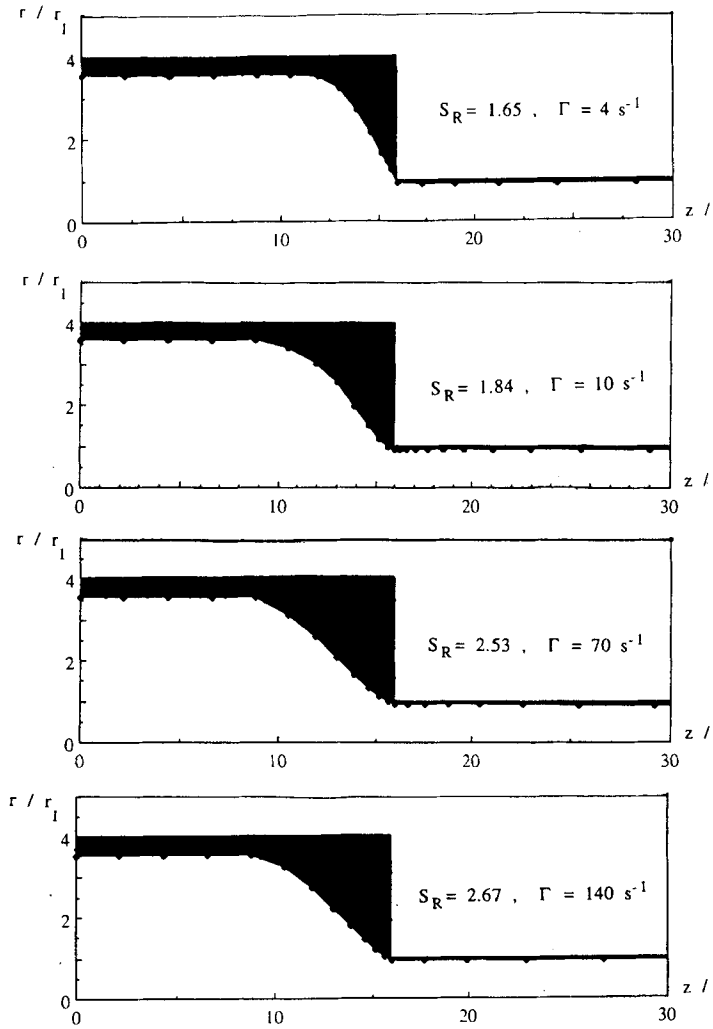

Figure 7. Computed limiting streamlines $\mathscr{L}^*$ showing the evolution of recirculating flow zones at various S_R-values

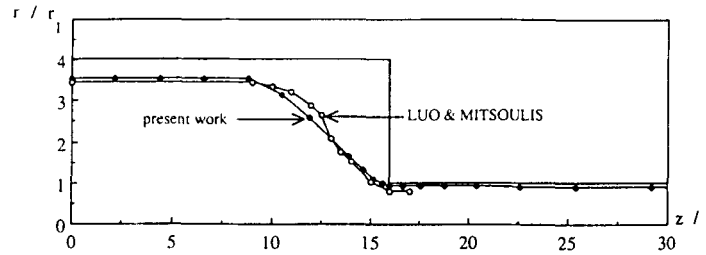

Figure 8. Comparison for S_R=2·53 between a computed streamline in the peripheral stream tube and a streamline determined from a finite element method in the total flow domain by Luo and Mitsoulis[7]

streamlines $\mathscr{L}^*$, starting at the same relative distance r^*/r_0 (r_0 is the radius of the upstream tube) are reported in Figure 11 and are found to coincide for the upstream sections close to the section of contraction. The stress peaks for the shear stress T^{13} (Figure 12(a)) and the stress difference $T^{33} - T^{11}$ (Figure 12(b)) along the first computed streamlines of the two contractions are found to be of the same order of magnitude. This result confirms the choice of the 4/1 contraction generally used in the literature for numerical simulation of viscoelastic flow.

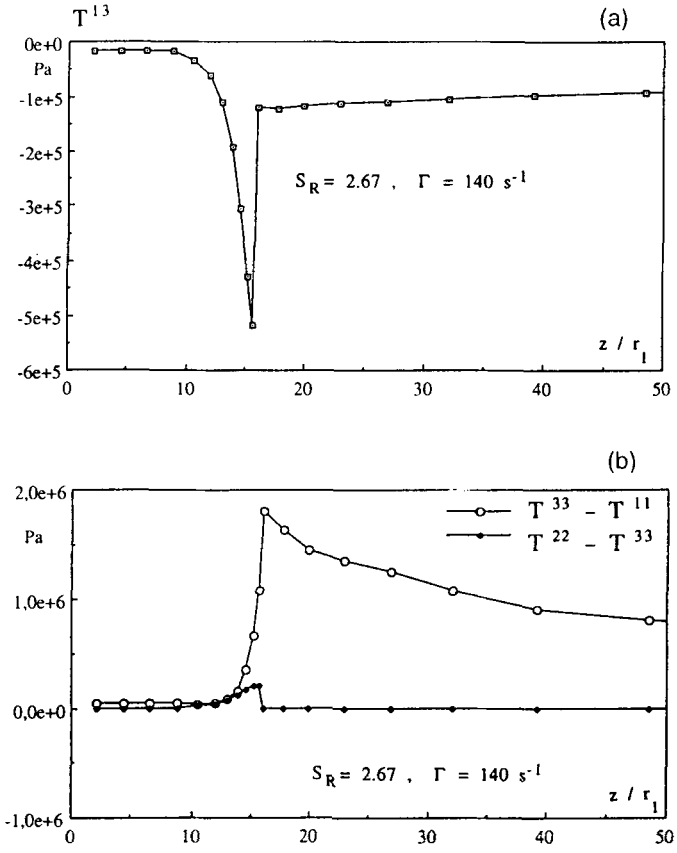

Figure 9. Stress distribution along the first computed streamline for S_R = 2·67: (a) shear stress T^{13}; (b) stress differences $T^{33} - T^{11}$ and $T^{11} - T^{22}$

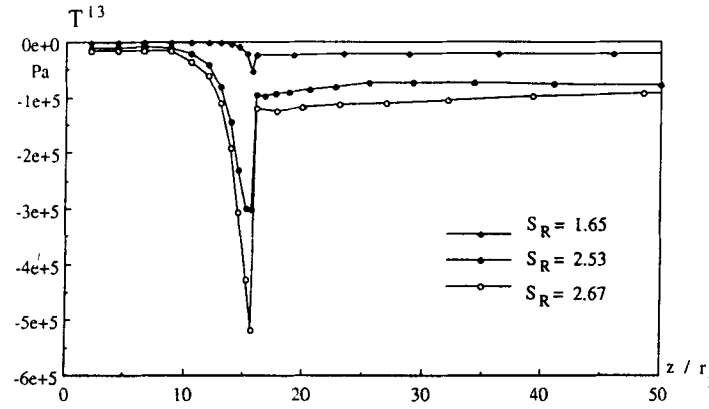

Figure 10. Stress component T^{13} for $S_R = 1{\cdot}65$, 2·53 and 2·67

7. CONCLUDING REMARKS

In this study the flow of a realistic memory integral fluid has been computed in abrupt axisymmetric 4/1 and 8/1 contractions. In the context of stream tube analysis the co-deformational K-BKZ model could be investigated in a simple way: the expressions for the kinematic tensors and the integral operators may be defined in a computational domain where the transformed lines of open streamlines are rectilinear and parallel, thus avoiding the problem of particle tracking. The complexity of the K-BKZ rheological model selected for computing the transformation function f led to a modified Hermite element being proposed. In relation to the multiple relaxation times of the constitutive equation, the lengths required for fully-developed Poiseuille flow to be obtained downstream of the contraction section were found to be greater than those indicated by using the single-integral Goddard–Miller equation previously considered in a 4/1 contraction.[16] As in the latter case, the approximating scheme and the Levenberg–Marquardt resolution algorithm led to consistent and stable numerical results even at high flow rates. By considering a peripheral stream-tube in the main flow region of the contraction, it was possible to evaluate wall effects on the stresses, even though the singularity at the salient corner was not explicitly taken into account when using the stream-tube method. The numerical results are satisfactory with regard to computed solutions in the literature, which require a resolution in the total flow domain.

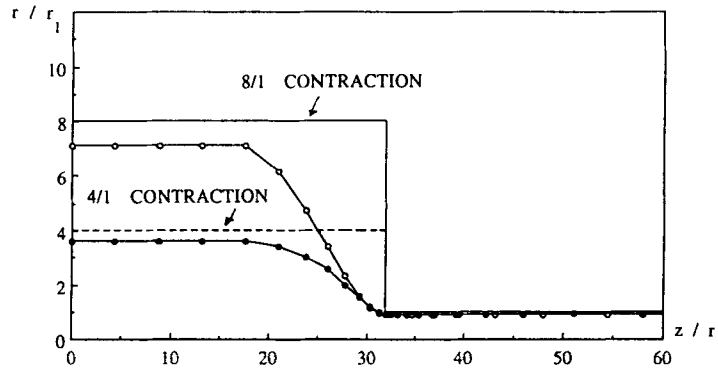

Figure 11. Comparisons of results for 4/1 and 8/1 axisymmetric contraction geometries, $S_R = 1{\cdot}84$: limited streamlines originating at the same relative abscissae at the upstream Poiseuille section

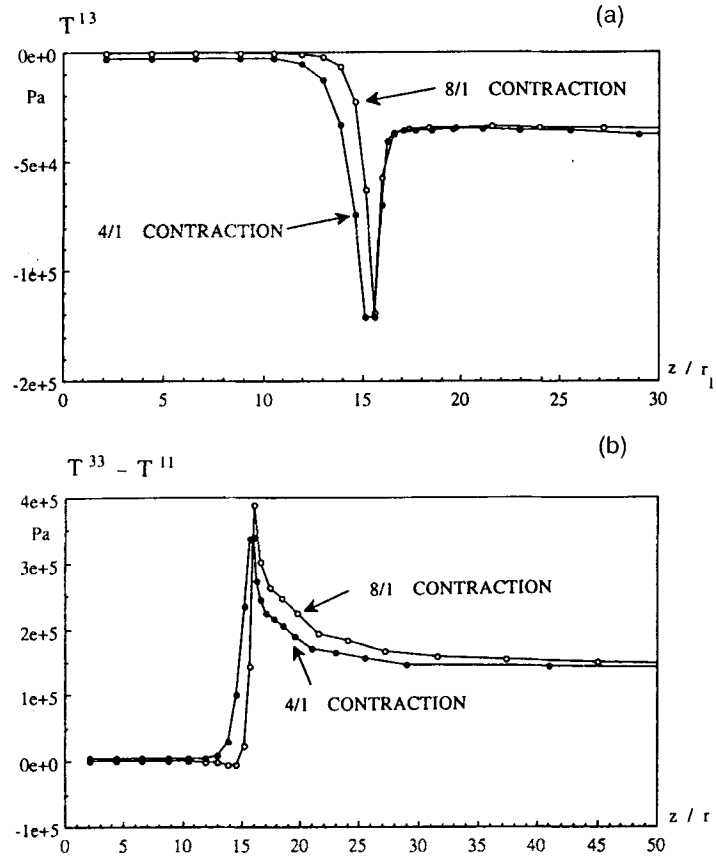

Figure 12. Comparisons of results for 4/1 and 8/1 axisymmetric contraction geometries, $S_R = 1{\cdot}84$: (a) stress component T^{13} along the first computed streamlines; (a) stress difference $T^{33} - T^{11}$ along the first computed streamlines

As pointed out previously, few theoretical results are available in the literature concerning the computation of complex flows with memory-integral equations. At the present time it is only possible to propose tentative explanations for the convergence of our method when using stream-tube analysis, as was done in a recent work.[16]

The present results confirm that it is possible to study complex flows with or without recirculation regions using the stream-tube method for various memory-type integral equations. The numerical solutions are obtained, with a very limited number of unknowns, using a computational algorithm which proved to be robust and efficient.

REFERENCES

1. M Viriyayuthakorn and B. Caswell, 'Finite element simulation of viscoelastic flow', *J. Non-Newtonian Fluid Mech.*, **6**, 245–267 (1980).
2. H. Court, K. Walters and R. Davies, 'Long-range memory effects in flows involving abrupt changes in geometry', *J. Non-Newtonian Fluid Mech.*, **8**, 95–117 (1981).
3. D. S. Malkus and B. Bernstein, 'Flow of a Curtiss–Bird fluid over a transverse slot using the finite-element drift function', *J. Non-Newtonian Fluid Mech.*, **16**, 77–116 (1984).
4. S. Dupont and M. J. Crochet, 'The vortex growth of a K-BKZ fluid in an abrupt contraction', *J. Non-Newtonian Fluid Mech.*, **16**, 82–91 (1988).

5. A. C. Papanastasiou, L. E. Scriven and C. W. Macosco, 'An integral constitutive equation for mixed flows: viscoelastic characterization', *J. Rheol.*, **27**, 387–410 (1983).
6. X. L. Luo and R. I. Tanner, 'Finite element simulation of long and short circular die extrusion experiments using integral models', *Int. j. numer. methods eng.*, **25**, 9–22 (1988).
7. X. L. Luo and E. Mitsoulis, 'An efficient algorithm for strain-history tracking in finite element computations of non-Newtonian fluids with integral constitutive equations', *Int. j. numer. methods fluids*, **11**, 1015–1031 (1990).
8. K. R. Rajagopal, 'Flow of viscoelastic fluids between rotating disks', *Theor. Comput. Fluid Dyn.*, **3**, 185–206 (1992).
9. A. C. Papanastasiou, L. E. Scriven and C. W. Macosco, 'A finite-element method for liquid with memory', *J. Non-Newtonian Fluid Mech.*, **22**, 271–288 (1987).
10. J. L. Duda and J. S. Vrentas, 'Fluid mechanics of laminar liquid jets', *Chem. Eng. Sci.*, **22**, 855–869 (1967).
11. K. Adachi, 'Calculation of strain histories in protean coordinate system', *Rheol. Acta*, **22**, 326–335 (1983).
12. K. Adachi, 'A note on the calculation of strain histories in orthogonal streamline coordinate systems', *Rehol. Acta*, **25**, 555–563 (1986).
13. J. R. Clermont, 'Sur la modelisation numérique d'écoulements plans et méridiens de fluides non-newtoniens incompressibles', *C.R. Adad. Sci. Paris (Sér. II.1)*, 297 (1983).
14. J. R. Clermont, 'Analysis of incompressible three-dimensional flows using the concept of stream tubes in relation with a transformation of the physical domain', *Rheol. Acta*, **27**, 357 (1988).
15. J. R. Clermont, M. E. de la Lande, T. Pham Dinh and A. Yassine, 'Analysis of plane and axisymmetric flows of incompressible fluids with the stream-tube method. Numerical simulation by a Trust–Region optimization algorithm', *Int. j. numer. methods fluids*, **13**, 371–399 (1991).
16. J. R. Clermont and M. E. de la Lande, 'Calculation of main flows of a memory-integral fluid at high Weissenberg numbers', *J. Non-Newtonian Fluid Mech.*, **46**, 89–110 (1993).
17. P. André and J. R. Clermont, 'Experimental and numerical study of the swelling of a viscoelastic liquid using the stream-tube method and a kinematic singularity analysis', *J. Non-Newtonian Fluid Mech.*, **39**, 1–29 (1990).
18. J. R. Clermont, 'Calculation of kinematic histories in two- and three-dimensional flows using streamline coordinate functions', *Rehol. Acta*, **32**, 82–93 (1993).
19. Y. Béreaux, *Rapport de DEA*, Université de Grenoble, 1992.
20. M. S. Chai and Y. L. Yeow, 'Modelling of fluid using multiple relaxation time constitutive equation', *J. Non-Newtonian Fluid Mech.*, **35**, 459–470 (1990).
21. B. D. Coleman, H. Markowitz and W. Noll. *Viscometric Flows of Non-Newtonian Fluids*, Springer, New York, 1966.
22. M. Normandin and J. R. Clermont, 'Numerical simulation of extrudate swell for Oldroyd-B fluids using the stream-tube analysis and a streamline approximation', *J. Non-Newtonian Fluid Mech.*, **50**, 193–215 (1993).
23. G. Touzot and G. Dhatt, *Une Présentation de la Méthode des Eléments Finis*, Editions Maloine, Paris, 1984.
24. A. Gourdin and M. Boumahrat, *Méthodes Numériques Appliquées, Technique et Documentation*, Editions Lavoisier, Paris, 1989.